PAPER • **OPEN ACCESS**

Cu_2FeSnS_4 nanoparticles: potential photovoltaic absorption materials for solar cell application

To cite this article: R Deepika and P Meena 2020 *Mater. Res. Express* **7** 035012

Materials Research Express

OPEN ACCESS

RECEIVED
6 November 2019

REVISED
22 February 2020

ACCEPTED FOR PUBLICATION
3 March 2020

PUBLISHED
16 March 2020

PAPER

Cu_2FeSnS_4 nanoparticles: potential photovoltaic absorption materials for solar cell application

R Deepika and P Meena

Department of Physics, PSGR Krishnammal College for Women, Coimbatore-641004, India

E-mail: drpmeena@gmail.com

Keywords: Cu_2FeSnS_4 (CFTS), facile chemical route method, Raman spectroscopy, optical absorption studies, electrochemical impedance spectroscopy analysis

Abstract

Quaternary semiconductor Cu_2FeSnS_4 (CFTS) nanoparticle powder have been prepared by a simple chemical technique. The synthesized CFTS nanoparticles have been characterized via powder XRD analysis, Raman spectra, FE-SEM-EDS, UV-Visible absorption spectroscopy, thermal analysis and electrochemical characterization. Powder XRD and Raman spectroscopy confirm the phase and structure of the prepared nanoparticles. The optical absorption studies reveal that the CFTS nanoparticles have a direct optimal band gap in the range from 1.32 to 1.5 eV, which indicates that these nanoparticles are potential absorber materials for thin-film photovoltaic application. The synthesized CFTS nanoparticles were transformed to the ink form and the obtained nanoparticle ink coated on a FTO conducting substrate (surface resistivity-13 Ω sq^{-1}). The catalytic activity of the substrate was analyzed by electrochemical impedance spectroscopy (EIS) and cyclic voltammogram (CV) curves. The appropriate optical band gap and stable electrical properties indicate that Cu_2FeSnS_4 Nanoparticles are potential materials for thin-film photovoltaic application.

1. Introduction

Considering the needs of the ever growing population, the demand for energy is expected to become twice in the ensuing decade. Conventional sources like fossil fuels (coal, natural fuel and gas) are being used up at a rapid pace. It is very essential to find other sources which are renewable, cheap and non-toxic. Among the various types of renewable energy, solar energy is highly attractive as it is sustainable, limitless and non-polluting. Solar cells harness the solar energy and convert it into electric energy.

Initially, more than 80% of the solar industry was based on silicon solar cells. Silicon based photovoltaic cells depend on the use of thick absorber materials with an indirect band gap. However, the materials used for these absorber layers are expensive [1].

Inorganic thin-film solar cell technology depends on direct band gap absorber materials like $CuInGaSe_2$ (CIGS) [2], $Cu_2ZnSn(S, Se)_4$ (CZTS) [3, 4], Cu_2FeSnS_4 (CFTS) [5], CdTe and TiO_2, which have been widely investigated for use in thin film solar cells. Being direct optical band gap, there is no need a thick absorber film. High power conversion efficiency has been achieved with these materials. However, these solar cells cannot be used expansively as they employ relatively rare and expensive elements like indium (In) and gallium (Ga). To attain the goal of low expenditure photovoltaic technology, it is required to analyze other semiconductor materials containing sulfur, which is low- noxious, as a replacement for selenium (Se) and iron which is available in plenty in the place of In and Ga [6]. CFTS nanoparticles are among the most promising nanomaterials for use as absorbers in thin film solar cells in view of the appropriate direct optimum band gap (Eg = 1.2 to 1.5 eV) and the profusely available and non-toxic elements [7–9].

Many vacuum and non- vacuum based systems have been developed to prepared CFTS nanomaterials. Physical techniques are expensive as their operation is difficult, and complex equipment and high vacuum are needed. On the other hand, chemical techniques are simple and cheap; there is low wastage of materials and no

need for vacuum, making them suitable for large scale production [10, 11]. Absorber nanomaterials show enhanced optical, chemical and mechanical properties in comparison to the bulk material. Nanomaterial technique ensures controlled nucleation and grain growth. The incorporation of dopants to control the chemical and structural properties can also been done easily. Hence, many efforts are being made to devise effective methods for the synthesis of the CFTS nanoparticles [12, 13].

Earlier researchers have used different techniques such as the solvothermal method [14], liquid reflux method [15], spray pyrolysis technique [16] and micro-wave irradiation method [17], for the preparation of the CFTS nanoparticles. In this present study, an effort has been made to prepare CFTS nanoparticles by the hydrothermal method as this technique is simple, eco-friendly, and cheap and can produce phase pure nanoparticles with high crystallinity. The precursor materials were first dissolved in the solvent and heated at the optimized time and temperature to produce the nanoparticles. The synthesized nanoparticles were dispersed in an environmentally benign solvent to produce a nanoparticle ink which was coated on ultrasonically cleaned FTO conducting glass substrates by the spin coating method [18]. Chemat KW 4A model spin- coating ensures uniformity of the thin film and produces good quality films suitable for photovoltaic applications.

2. Materials and methods

2.1. Preparation of Cu_2FeSnS_4 nanoparticles

The cationic precursors, copper (II) chloride ($CuCl_2.2H_2O$), iron (II) chloride ($FeCl_2.4H_2O$) and tin (II) chloride dehydrate ($SnCl_2.2H_2O$) and the anionic precursor, thiourea (CH_4N_2S), all of 99.9% purity, were procured from Sigma Aldrich chemicals.

An aqueous solution of the cationic precursors (0.02M of $CuCl_2.2H_2O$, 0.008M of $FeCl_2.4H_2O$ and 0.002M $SnCl_2.2H_2O$) was prepared by adding them in distilled water in the above sequence, allowing adequate interval to dissolve the solute. The anionic precursor thiourea (0.04 M) was next mixed in the above aqueous solution. The mixture was vigorously stirred for 3 h and ultrasonicated for 30 min to homogenize the solution. The obtained solution was shifted into 50 ml capacity of stainless steel autoclave and retained at 190 °C for 24 h. The obtained product was centrifuged and washed repeatedly using water and ethanol, and then dried at 90 °C for 7 h, before being used for characterization.

To convert the powder into the thin film form it was dissolved in ethanol and grinding for 3 h to get a homogeneous slurry, which was spin-coated on the FTO substrate at a 2000 rpm speed for 30 s. The obtained thin film was heated using a hot plate at 150 °C for 10 min to eliminate the solvent. The spin - coating and drying process for several times to obtain the required thickness. The resultant thin-film was annealed by 400 °C intended for 30 min to obtain the CFTS absorbance layer.

2.2. Material characterization

Powder XRD study was carried out using the Panalytical XPERT Pro (Netherlands) x-ray diffraction system with Cu-Kα radiation source (wavelength $=$ 1.5406 Å) operated at 45 kV. The XRD powder patterns were obtained in the scanning range of $2\theta = 10°$–$90°$ at a scanning rate maintained at $2°$ min^{-1}. The micro- Raman spectra were obtained by using a 'WiTec alpha 300' Raman microscope (Germany) in the Raman Spectral range from 50 to 4000 cm^{-1}. The synthesized nanoparticles was studied by FE-SEM using the S4160 Hitachi equipment and the chemical composition analyzed by Bruker-4010 model EDS analyzer. The optical UV–vis- NIR spectra were studied using a JASCO (model V-770) UV–vis- NIR spectrophotometer. Electrochemical measurement was done using the electrochemical workstation.

3. Result and discussion

3.1. Structural analysis

The crystalline structure of the Cu_2FeSnS_4 nanoparticle and its phase were analyzed by powder XRD studies. Figure 1 shows the powder XRD peak positions of hydrothermally prepared nanoparticles. The CFTS powder showed strong diffraction peaks correspond to $\langle 112\rangle$, $\langle 200\rangle$, $\langle 201\rangle$ and $\langle 312\rangle$ planes. These are in good agree with the JCPDS card number: PDF 44 - 1476 in the tetragonal space group $\langle I\text{-}42m\rangle$. These results agree with reports in previous literature [19, 20]. The lattice parameters for the tetragonal structure were estimated using the relation,

$$\frac{1}{d^2} = \frac{h^2 + k^2}{a^2} + \frac{l^2}{c^2} \quad (1)$$

L

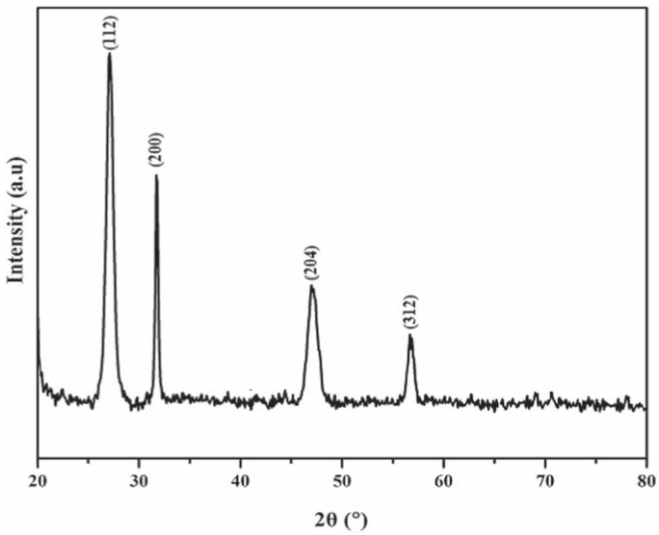

Figure 1. Powder XRD spectrum for CFTS nanoparticles.

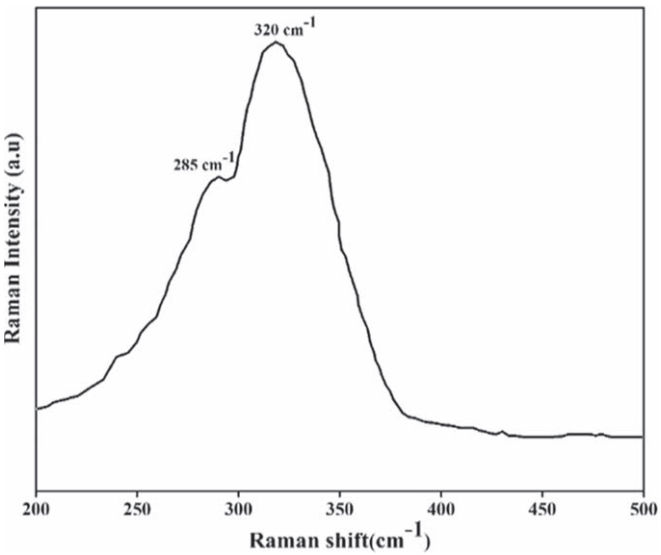

Figure 2. Raman spectrum for CFTS nanoparticles.

Where, d is the interplanar spacing and h, k and l are the Miller indices. The lattice parameters were calculated to be a = b = 5.55 Å and c = 10.76 Å which agree with the JCPDS card values a = b = 5.43 Å and c = 10.73 Å. The crystallite size was estimate by using the Scherrer's formula,

$$D = \frac{k\lambda}{\beta \cos \theta} \tag{2}$$

Where, D is the grain size, k is the constant $\langle 0.9 \rangle$, λ is the x-ray wavelength radiation and β is the FWHM of the peak. The mean crystallite sizes of the synthesized nanoparticles were calculated to be within the range from 8 to 30 nm.

3.2. Raman spectroscopy analysis

In order to confirm the phase and crystal structure of the CFTS absorber material, Raman spectrum of the nanoparticles were recorded and are shown in figure 2. The micro- Raman spectroscopy assist in identifying the secondary phases and confirms the phase purity of the CFTS absorber powder material. Miao *et al* [10] have obtained Raman peaks at 318 and 284 cm^{-1} which are due to the CFTS nanoparticles. The peak obtained at 372 cm^{-1} is ascribed to $Cu_2Sn_3S_7$ (CTS) nanoparticles. The strong peak obtained at 318 cm^{-1} indicates the good crystalline structure of the film. Chatterjee *et al* [11] have shown a conspicuous peak at 320.9 cm^{-1}, which is

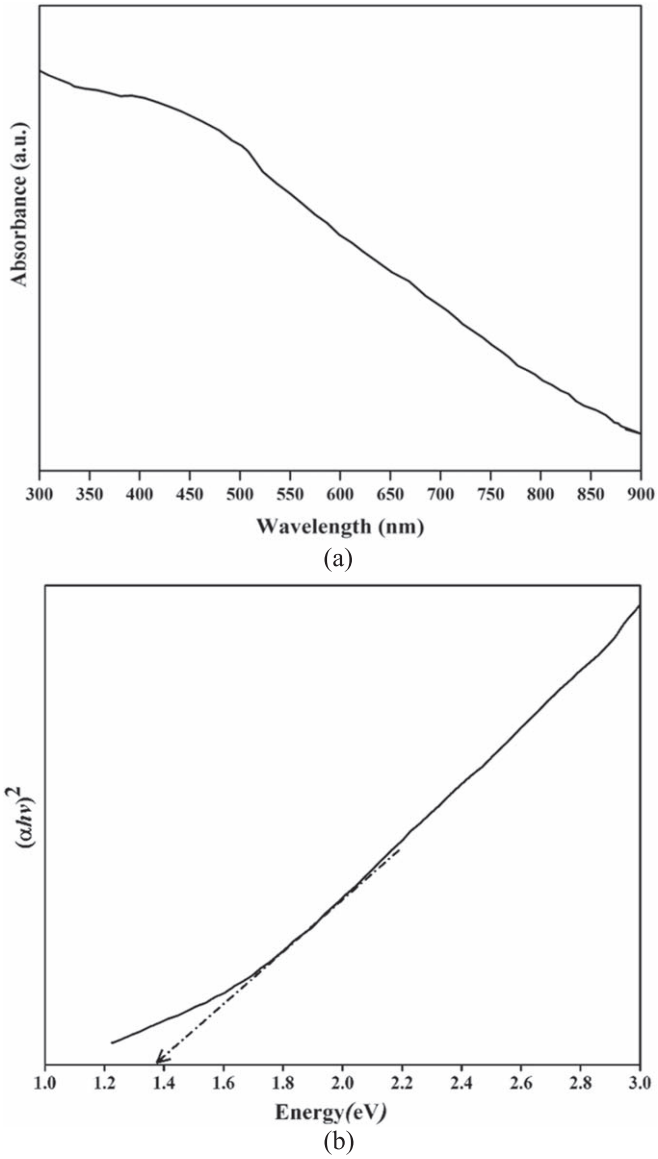

Figure 3. (a). Absorption spectrum of CFTS nanoparticles. (b). The plot of $h\upsilon$ versus $(\alpha h\upsilon)^2$ for CFTS nanoparticles.

attributed to the strong asymmetry vibration of the pure-anion mode of the sulfur atoms around the tin metal. This also confirms the phase purity of CFTS absorber nanomaterials. Vanalakar *et al* [21] have shown secondary impurity peaks at 293, 319, 332,352 and 492 cm^{-1} corresponding to FeS, Cu_2FeSnS_4, Cu_2SnS_4, Cu_2FeS_4 and FeS respectively. The Raman spectra show impurity peaks and the most intense peak is seen at about 319 cm^{-1} which is attributed to the characteristic mode of Cu_2FeSnS_4.

From figure 2, it is observed that the strongest peak is at 320 cm^{-1} and an additional shoulder peak is at 285 cm^{-1} which confirm the specific vibration mode of the CFTS quaternary semiconductor material. The strong peak at 320 cm^{-1} is attributed to the A_1 symmetric vibrational motion of sulfur atoms in CFTS, and the shoulder peak to the pure anion-mode of the sulfur atoms around the copper cation, indicating that the powder has good crystallinity and phase pure CFTS has been obtained, confirming the XRD results.

3.3. UV–vis-NIR spectral analysis

To understand the optical absorbance properties of the synthesized CFTS powder, the UV-spectrum is recorded in the DRS mode in the wavelength ranging from 250–900 nm. The UV spectra obtained are shown in figure 3(a). It is observed that the prepared Cu_2FeSnS_4 nanoparticles exhibit a wide absorption in the UV visible region with absorption tails that extend into longer wavelength region. The optical band gap of the CFTS nanoparticles was estimated from a plot of $(\alpha h\upsilon)^2$ as a function of $h\upsilon$, where α is the absorbance, h is the Planck's constant and υ is the frequency. Here $(\alpha h\upsilon) = A(h\upsilon - Eg)^n$, where Eg (eV) is the optical band gap energy and $n = \frac{1}{2}$ for direct optical Eg semiconductor. The optical Eg was determined to be approximately 1.39 eV by extra

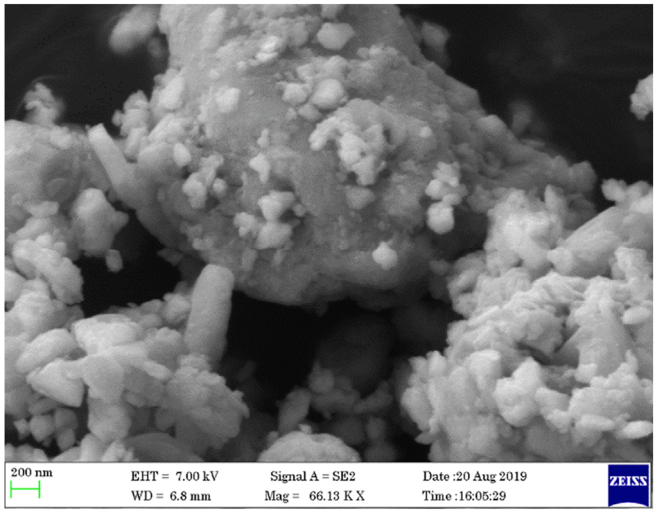

(a)

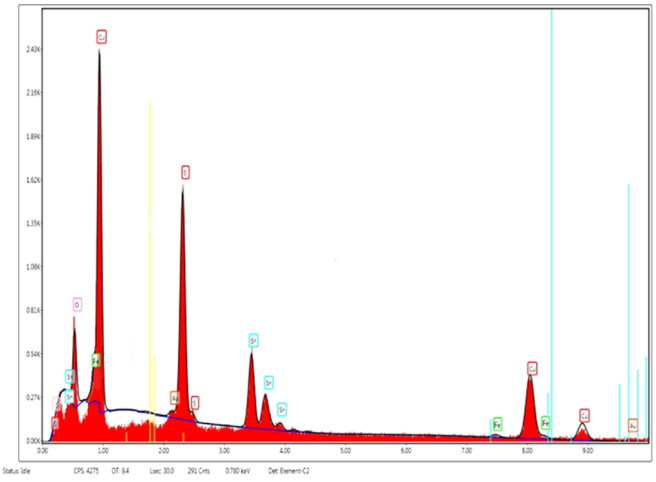

(b)

Figure 4. (a). SEM image for CFTS nanoparticles. (b). EDS spectra of CFTS nanoparticles.

plotting the linear part of the spectrum to zero as in figure 3(b). This is close to the optimum value for high conversion efficiency [22, 23].

3.4. Morphological and compositional analysis

The FE-SEM image of the CFTS nanoparticles is shown in figure 4(a). The CFTS nanoparticles reveal slight agglomeration with irregular sphere like particle average size from 10–30 nm, which agrees with the XRD data. This slight agglomeration could be attributed to an increase in surface energy with decrease in size [24]. This kind of sphere like morphology enhances photon absorption and hence finds use in photovoltaic applications.

The EDS spectrum in figure 4(b) indicates peaks corresponds to copper, iron, tin and thiourea, endorsing the phase purity of the Cu_2FeSnS_4 nanoparticles. The elemental composition ratio of copper, iron, tin and thiourea in Cu_2FeSnS_4 is about 29.82: 15.93: 3.78: 50.47, which is close to the initial starting material [25].

3.5. Thermal analysis

Thermal analysis using TGA and DSC was done to study the various phase transformations. The obtained TGA and DSC curves are shown in figures 5(a) and (b). From the TGA plot, it observed that the first loss occurs from 80 °C to 100 °C. This ascribed to the decomposition of the Cu-Fe-Sn-thiourea-oxygen complex to form CFTS and other organic solvents. The second weight loss starting from 280 °C and ending at 540 °C can be due to the oxidation of the sulfides; above 320 °C is comparatively slow oxidation of sulfides due to loss of weight. A substantial weight loss is observed in the third region because of the calcination of structural water which is eliminated below 300 °C. In the final region, the sample is nearly stable without any weight loss. The DSCcurve shows an exothermic peak ranging from 380 °C–430 °C which shows the crystallization of the synthesized powder. The decomposition in Cu-Fe-Sn-S _ oxides compound under a slow atmosphere indicates to the

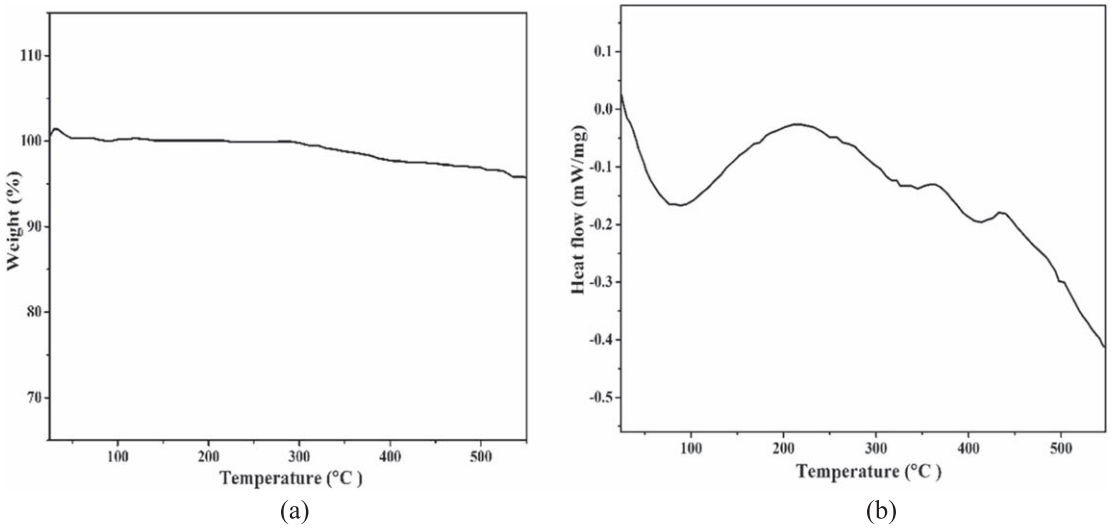

Figure 5. (a). TGA and 5(b). DSC curves for CFTS nanoparticles.

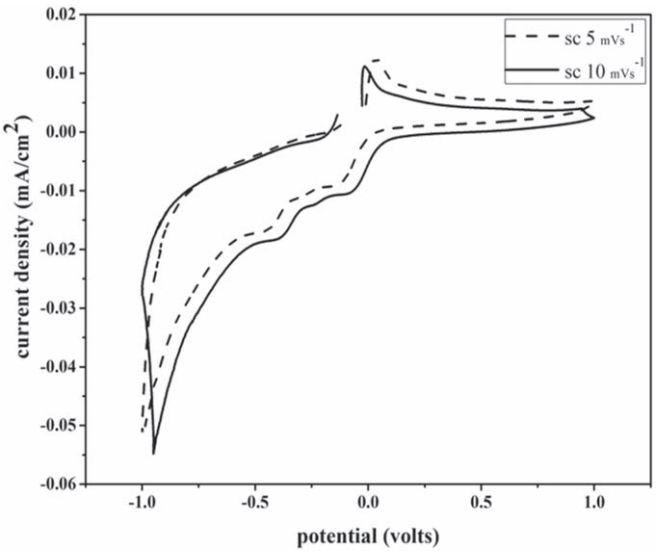

Figure 6. CV curve for CFTS annealed CFTS thin film.

lessening of oxidation state. Decomposition under an oxygen atmosphere is more suitable to reduce oxidize the C-N or C-H bonds in the carbon-based solvents [26].

3.6. Cyclic voltammogram (CV) measurements

To study the electro catalytic ability of the annealed Cu_2FeSnS_4 thin-films was evaluated by cyclic voltammetry measurements were performed under three electrode system with 0.1M NaOH electrolyte in the potential ranging from −1.0 V − 1.0 V with scan rates (sc) of 5 and 10 mVs^{-1}. FTO glass was used as the working electrode slurry was spin-coated onto the FTO substrate <1 cm × 1 cm> while platinum wire and Ag/AgCl were employed as the counter and reference electrodes. From figure 6, it is observed that for a 5 mVs^{-1} scan rate, the anodic peak is observed at 0.012 mA cm^{-2} and cathodic peaks at − 0.0087 mA cm^{-2} and −0.0154 mA cm^{-2}. The corresponding potentialof the anodic peak is at 0.0518 V and that of the cathodic peaks are at −0.135 V and −0.4195 V respectively.

For a 10 mVs^{-1} scan rate, the maximum current density peaks were detected at 0.0109 mA cm^{-2} (anodic peak) and −0.0095 mA cm^{-2} and −0.0179 mA cm^{-2} (cathodic peaks). The corresponding potential of the anodic peak is 0.0085 V and the cathodic peak potentials are −0.049 V and −0.385 V respectively (figure 6). It is observed that the area under the CV curve increased with the scan rate. The cathodic peak at maximum current

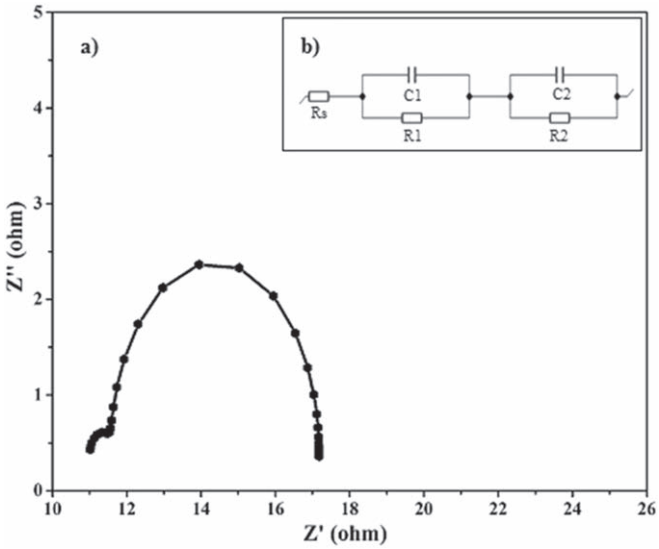

Figure 7. (a) EIS spectra: Nyquist plot and 7(b). Equivalent circuit for annealed CFTS thin film.

density indicates an electrochemical behavior and good catalytic activity of the annealed CFTS in NaOH electrolyte.

Anima Ghosh *et al* [27] have reported that the cyclic voltammetric curves for copper based chalcogenide thin films show a rise in the current density when illuminated visible light. These films are used in photo-electrochemical applications. Shanlong Chen *et al* [28] have shown that the CV curves of CZTS CEs (counter electrode) display cathodic peaks. The analogous nature of the curves for Cu_2ZnSnS_4 and Platinum CEs indicates similar electro chemical activities.

3.7. Electrochemical impedance spectroscopy (EIS) analysis: nyquist plot

EIS: Nyquist plot study was used to investigate the catalytic action of the CFTS film. The impedance plot (Nyquist plot) was obtained by plotting the real part (Z′) against the imaginary part (Z″).

The Nyquist plots under illumination in the frequency ranging from 100 kHz − 10 mHz with an amplitude of 5 mV is shown in figure 7(a) for the annealed CFTS thin film. The equivalent circuit as shown in the inset of figure 7(b). Rs (series resistance) is the equivalent circuit in the electrode system. Rct (charge transfer resistance) is due to the high- frequency range in the semcircle. Electrolyte-electrode interfaces in the CPE (corresponding constant phase angle element). Inset shows the figure 7(b), charge transfer—resistance and twin layer capacitance at the electrode- electrolyte interfaces (R1,C1), the recombination charge transmission resistance and capacitance at the electrode-electrolyte interfaces (R2 , C2) respectively. In previous literature, Chen *et al* [29] have shown that a small Rs value ensures good binding between the film and the FTO substrate and the CTS (Cu_2SnS_3) material exhibits higher catalytic activity. Mokurala *et al* [30], have shown that a smaller R_{ct} value specifies the capable for quicker electro-catalytic lessening of ions in the electrolyte. A marginally higher Rs value is due to the reduced binding strength of the thin film to conducting glass (FTO).

From figure 7(a) it is observed that, R_s and R_{ct} exhibit values of 10.81 Ω and 5.4 Ω respectively for the annealed CFTS film electrode. R_{ct} is responsible for the increase in the catalytic activity of the annealed CFTS film. According to earlier researchers [29, 30], a good electrocatalytic activity characteristic was also observed in the dense CFTS film prepared by spin-coating. This agrees with the results obtained from the EIS and CV curves. The optimized CFTS thin films exhibit good photovoltaic performance and electrochemical properties which make them suitable for solar cell applications.

4. Conclusion

Copper iron tin thiourea nanoparticles were prepared by a simple chemical route technique. XRD studies revealed that CFTS nanoparticles have a tetragonal structure. The formation of tetragonal space group I-42m is confirmed by Raman spectroscopy. The synthesized CFTS nanoparticles are found to have an optical Eg is 1.39 eV makes them potential to use as an absorber layer in photovoltaic application. Morphological studies show that the average size of the prepared nanoparticles in the range from 10–30 nm and show slight agglomeration with irregular sphere like particles. The phase transformation and annealing temperature were determined by

TGA and DSC thermal analysis. The cyclic voltammetry measurements show the electro-catalytic of the annealed Cu_2FeSnS_4 thin-film electrodes. Electrochemical impedance spectroscopy results show good electro-catalytic and lesser charge transferal resistance to the electrode - electrolyte interfaces. On the beginning of the CV curves and Nyquist plot, improved performance of the annealed CFTS thin films is observed which is ascribed to the superior catalytic activity of CFTS in NaOH solution. The obtained results indicate that quaternary CFTS nanoparticles and annealed thin films exhibit the potential for use as absorber layers in solar cell applications.

ORCID iDs

R Deepika https://orcid.org/0000-0002-7222-0040

References

[1] Mitzi D B, Yuan M, Liu W, Kellock A J, Chey S J, Deline V and Schrott A G 2008 A high-efficiency solution-deposited thin-film photovoltaic device *Adv. Mater.* **20** 3657–62
[2] Meng X, Deng H, Sun L, Yang P and Chu J 2015 Sulfurization temperature dependence of the structural transition in Cu_2FeSnS_4-based thin films *Mater. Lett.* **161** 427–30
[3] Fernandes P A, Salomé P M P and Da Cunha A F 2011 Study of polycrystalline Cu_2ZnSnS_4 films by Raman scattering *J. Alloys Compd.* **509** 7600–6
[4] Vanalakar S A, Agawane G L, Kamble A S, Patil P S and Kim J H 2017 The green hydrothermal synthesis of nanostructured $Cu_2ZnSnSe_4$ as solar cell material and study of their structural, optical and morphological properties *Appl. Phys.* A **123** 782
[5] Wang S, Ma R, Wang C, Li S and Wang H 2017 Incorporation of Rbcations into Cu_2FeSnS_4 thin films improves structure and morphology *Mater. Lett.* **202** 36–8
[6] Nilange S G, Nandkishor M P and Yadav A A 2019 Growth and characterization of spray deposited quaternary Cu_2FeSnS_4 semiconductor thin films *Physica.* B **560** 103–10
[7] Agawane G L, Shin S W, Vanalakar S A, Moholkar A V and Kim J H 2014 Next generation promising Cu2 (ZnxFe1− x) SnS4 photovoltaic absorber material prepared by pulsed laser deposition technique *Mater. Lett.* **137** 147–9
[8] Agawane G L, Vanalakar S A, Kamble A S, Moholkar A V and Kim J H 2018 Fabrication of Cu2 (ZnxMg1-x) SnS4 thin films by pulsed laser deposition technique for solar cell applications *Mater. Sci. Semicond. Process.* **76** 50–4
[9] Vanalakar S A, Patil P S and Kim J H 2018 Recent advances in synthesis of Cu2FeSnS4 materials for solar cell applications: a review *Sol. Energy Mater. Sol. Cells* **182** 204–19
[10] Miao X, Chen R and Cheng W 2017 Synthesis and characterization of Cu_2FeSnS_4 thin films prepared by electrochemical deposition *Mater. Lett.* **193** 183–6
[11] Chatterjee S and Amlan J P 2017 A solution approach to p-type Cu_2FeSnS_4 thin-films and pn-junction solar cells: role of electron selective materials on their performance *Sol. Energy Mater. Sol. Cells* **160** 233–40
[12] Lydia R and Sreedhara Reddy P 2013 Effect of pH on the characteristics of Cu_2ZnSnS_4 nanoparticles ISRN *Condens. Matter Phys.* **2013** 5
[13] Belaqziz M, Medjnoun K, Djessas K, Chehouani H and Grillo S E 2018 Structural and optical characterizations of Cu_2SnS_3 (CTS) nanoparticles synthesized by one-step green hydrothermal route *Mater. Res. Bull.* **99** 182–8
[14] Nazari P, Yazdani A, Shadrokh Z, AbdollahiNejand B, Farahani N and Seifi R 2017 Band gap engineering of $Cu_3FexSn_{(1-x)}S_4$: a potential absorber material for solar energy *J. Phys. Chem. Solids* **111** 110–4
[15] Zhou J, Ye Z, Wang Y, Yi Q and Wen J 2015 Solar cell material Cu_2FeSnS_4 nanoparticles synthesized via a facile liquid reflux method *Mater. Lett.* **140** 119–22
[16] El Fidha G, Bitri N, Mahjoubi S, Abaab M and Ly I 2018 Effect of the spraying temperatures and the sulfurization on the properties of the absorber Cu_2FeSnS_4 thin films in a solar cell *Mater. Lett.* **215** 62–4
[17] Guan H, Shi Y, Jiao B, Wang X and Yu F 2014 Flower-like Cu_2FeSnS_4 particles synthesized by microwave irradiation method *Chalcogenide Lett.* **11** 9–12
[18] Liu W, Guo B, Mak C, Li A, Wu X and Zhang F 2013 Facile synthesis of ultrafine Cu2ZnSnS4 nanocrystals by hydrothermal method for use in solar cells *Thin Solid Films* **535** 39–43
[19] Adelifard M 2016 Preparation and characterization of Cu_2FeSnS_4 quaternary semiconductor thin films via the spray pyrolysis technique for photovoltaic applications *J. Anal. Appl. Pyrolysis* **122** 209–15
[20] Jiang X, Xu W, Tan R, Song W and Chen J 2013 Solvothermal synthesis of highly crystallized quaternary chalcogenide Cu_2FeSnS_4 particles *Mater. Lett.* **102** 39–42
[21] Vanalakar S A, Patil S M, Patil V L, Vhanalkar S A, Patil P S and Kim J H 2018 Simplistic eco-friendly preparation of nanostructured Cu_2FeSnS_4 powder for solar photocatalytic degradation *Materials Science and Engineering:* B **229** 135–43
[22] Cao M, Li C, Zhang B, Huang J, Wang L and Shen Y 2015 PVP assisted solvothermal synthesis of uniform Cu_2FeSnS_4nanospheres *J. Alloys Compd.* **622** 695–702
[23] Zhou J, Yu S, Guo X, Wu L and Li H 2019 Preparation and characterization of Cu_2FeSnS_4 thin films for solar cells via a co-electrodeposition method *Curr. Appl. Phys.* **19** 67–71
[24] Phaltane S A, Vanalakar S A, Bhat T S, Patil P S, Sartale S D and Kadam L D 2017 Photocatalytic degradation of methylene blue by hydrothermally synthesized CZTS nanoparticles *J. Mater. Sci., Mater. Electron.* **28** 8186–91
[25] Wang W, Shen H, Yao H and Li J 2014 Preparation and properties of Cu_2FeSnS_4nanocrystals by ultrasound-assisted microwave irradiation *Mater. Lett.* **125** 183–6
[26] Su Z, Sun K, Han Z, Cui H, Liu F, Lai Y, Li J, Hao X, Liu Y and Green M A 2014 Fabrication of Cu_2ZnSnS_4 solar cells with 5.1% efficiency via thermal decomposition and reaction using a non-toxic sol–gel route *J. Mater. Chem.* A **2** 500–9
[27] Ghosh A, Chaudhary D K, Biswas A, Thangavel R and Udayabhanu G 2016 Solution-processed Cu_2XSnS_4 (X = Fe, Co, Ni) photo-electrochemical and thin film solar cells on vertically grown ZnOnanorod arrays *RSC Adv.* **6** 115204–12
[28] Chen S, Xu A, Tao* J, Tao* H, Shen Y, Zhu L, Jiang J, Wang T and Pan L 2015 *In-situ* and green method to prepare Pt-free Cu_2ZnSnS_4 (CZTS) counter electrodes for efficient and low cost dye-sensitized solar cells *ACS Sustainable Chemistry & Engineering.* **3** 2652–9

[29] Chen S-L, Tao J, Shu H-B, Tao H-J, Tang Y-X, Shen Y-Z, Wang T and Pan L 2017 Efficient electron transfer kuramite Cu_3SnS_4nanosheet thin film towards platinum-free cathode in dye-sensitized solar cells *J. Power Sources* **341** 60–7
[30] Mokurala K, Mallick S and Bhargava P 2016 Alternative quaternary chalcopyrite sulfides (Cu_2FeSnS_4 and Cu_2CoSnS_4) as electrocatalyst materials for counter electrodes in dye-sensitized solar cells *J. Power Sources* **305** 134–43